Identifying Resting-State Networks and Noise in rs-fMRI Using Visual Classification of ICA Components

Giuseppe Legista
Università Politecnica delle Marche (UNIVPM)
Ancona, Italy
S1114384@studenti.univpm.it

Mauro Silveri
Università Politecnica delle Marche (UNIVPM)
Ancona, Italy
S1114536@studenti.univpm.it

Davide Pitucci
Università Politecnica delle Marche (UNIVPM)
Ancona, Italy
S1114470@studenti.univpm.it

Christian Di Salvo
Univeristà Politecnica delle Marche (UNIVPM)
Ancona, Italy
S1114425@studenti.univpm.it

***Abstract*—Resting-state functional magnetic resonance imaging (rs-fMRI) allows the investigation of the brain's intrinsic functional architecture by analyzing spontaneous low-frequency fluctuations in the BOLD signal. Independent Component Analysis (ICA) is widely used to decompose rs-fMRI data into distinct spatial components, but the accurate classification of neural signals versus noise remains essential. In this study, rs-fMRI data from the Yale Resting State fMRI/Pupillometry study were processed with FSL and decomposed using MELODIC. Manual classification of 49 extracted components was performed based on spatial, temporal, and spectral characteristics, following Griffanti et al. guidelines. The spatial maps were validated by comparison with Smith et al. canonical resting-state networks. Ten components matched known networks, including the medial and lateral visual areas, default mode, sensorimotor, auditory, and frontoparietal networks. Noise components were identified based on features indicative of motion artefacts, physiological noise, and scanner-related disturbances. This work emphasizes the importance of rigorous component evaluation to ensure reliable resting-state fMRI analysis.**

Keywords—Resting-state fMRI, Independent Component Analysis, BOLD signal, Functional connectivity, Noise classification

I. INTRODUCTION

Resting-state functional magnetic resonance imaging (rs-fMRI) is a powerful neuroimaging technique that enables the investigation of the brain's intrinsic functional architecture by capturing spontaneous, low-frequency fluctuations in the blood-oxygen-level-dependent (BOLD) signal. These fluctuations reflect synchronized neural activity across distributed brain regions, revealing resting-state networks (RSNs) such as the default mode, visual, auditory, sensorimotor, and frontoparietal networks [1, 5]. The BOLD signal, which underpins fMRI, is sensitive to changes in blood oxygenation associated with neuronal activity. However, BOLD-based measurements are also susceptible to a variety of noise sources, including physiological processes (e.g., cardiac and respiratory cycles), subject movements, and scanner-related artifacts such as magnetic field inhomogeneities or gradient distortions [2, 3, 6]. These confounding factors can disturb the useful neural signals readings and must be addressed to ensure accurate functional connectivity analysis. Independent Component Analysis (ICA) has become a standard technique for processing rs-fMRI data. As a blind source separation method, ICA decomposes the observed fMRI signal into a set of statistically independent spatial components and their associated time courses. The classification of ICA components into signal or noise relies on the evaluation of three key features: spatial maps, temporal dynamics, and power spectral density. Spatially, signal components typically manifest as large, coherent clusters primarily confined to grey matter regions and often resemble known resting-state networks (RSNs) with symmetrical and anatomically plausible patterns. In contrast, noise components tend to appear as fragmented or scattered clusters located in white matter, cerebrospinal fluid (CSF) spaces, or near large blood vessels. Temporally, signal components are characterized by smooth, slowly varying time courses with minimal abrupt changes, whereas noise components often display sudden spikes or drifts in their time series. Regarding the frequency domain, the power

spectral density (PSD) of signal components is usually dominated by low-frequency power below 0.1 Hz, reflecting the typical temporal characteristics of spontaneous neural fluctuations. Noise components, by contrast, often exhibit atypical spectral profiles, with higher frequency contributions or irregular patterns inconsistent with genuine neural activity. Griffanti et al. [2] formalized these principles into a structured visual classification protocol for ICA components, which remains the gold standard for small or heterogeneous datasets. Although automated algorithms like FIX [3] and ICA-AROMA incorporate these features into machine learning classifiers, manual inspection remains essential for validating component classification and identifying edge cases that may be misclassified by automated systems. The relevance of ICA-derived RSNs has been independently validated by Smith et al. [1], who demonstrated that RSNs identified in resting-state data strongly correspond to the networks activated during a wide range of task-based paradigms. This confirms the biological significance of the spatial components isolated by ICA, strengthening the rationale for rigorous component selection and denoising.

II. MATERIALS AND METHODS

This study used resting-state functional MRI (rs-fMRI) data from the *Yale Resting State fMRI/Pupillometry: Arousal Study*, available on the OpenNeuro platform [1]. The dataset includes high-resolution structural and functional scans from healthy adult participants. For the purposes of this analysis, only the second resting-state run from each subject was used. All imaging data were acquired using a Siemens 3 Tesla Prisma scanner equipped with a 64-channel HeadNeck coil at the Yale University Magnetic Resonance Research Center. The structural T1-weighted images were obtained using a 3D MPRAGE sequence with a repetition time (TR) of 2400 ms, echo time (TE) of 1.22 ms, inversion time of 1000 ms, and a flip angle of 8°. The images had an isotropic voxel size of 1×1×1 mm^3 and a slice thickness of 1 mm. Functional BOLD imaging was conducted using a 2D multiband EPI sequence with a TR of 1000 ms, TE of 30 ms, a flip angle of 55°, and a multiband acceleration factor of 5. The voxel resolution was 2×2×2 mm^3, and a slice thickness of 2 mm with no gap between slices, with 410 volumes acquired over approximately 6 minutes and 50 seconds. Each volume contained 75 slices aligned along the anterior–posterior commissure (AC–PC) plane. All preprocessing was performed using FSL version 6.0, primarily through the FEAT graphical user interface. Before any formal processing, a data quality check was conducted to ensure consistency across key metadata parameters, such as repetition time, number of volumes, and voxel dimensions, to prevent incompatibilities during batch analysis. The anatomical images were first processed with FSL's Brain Extraction Tool (BET) to remove non-brain tissues. Several threshold values were tested, and 0.33 was selected for the fractional intensity one as the most appropriate based on visual inspection in FSLeyes, along with the gradient threshold setted to 0.33. The skull-stripped anatomical image was later used to guide alignment with functional data and to improve normalization to standard space. Slice timing correction was not applied to the input data, maintaining FSL's default setting. Head motion correction was performed using MCFLIRT, FSL's motion correction algorithm, which aligns all functional volumes to a reference volume using rigid-body transformation. The estimated translation and rotation parameters were visually inspected through motion plots to identify any significant movement or outlier volumes. When loading the input data, the first 10 volumes of the run were removed, to avoid the introduction of possible artifacts related to the start of the acquisition process. Temporal filtering was applied to remove low-frequency drifts from the time series, a process known as detrending. Specifically, a high-pass filter with a cutoff of 100 seconds (0.01 Hz) was used. No low-pass filter was applied, in order to preserve physiologically relevant high-frequency components of the BOLD signal that could otherwise be distorted. Spatial smoothing was applied using a Gaussian kernel with a full width at half maximum (FWHM) of 6 mm. This step increases the signal-to-noise ratio and accounts for minor anatomical variability across participants by averaging each voxel's signal with those of its neighbors. Functional data were co-registered to the individual's anatomical

image and subsequently normalized to the MNI152 2 mm standard space. Co-registration and normalization were performed as a combined process in the FEAT "Registration" tab. An affine transformation with 12 degrees of freedom was used, and the quality of alignment was visually assessed using FSLeyes. Following preprocessing, spatial Independent Component Analysis (ICA) was conducted using MELODIC (Multivariate Exploratory Linear Optimized Decomposition into Independent Components) version 3.0. MELODIC decomposed the four-dimensional fMRI dataset into spatially independent components and their corresponding time courses. The dimensionality of ICA was automatically estimated, and the resulting spatial maps were thresholded using a z-score cutoff of 0.35. Each component extracted by ICA was then manually classified as either signal or noise based on guidelines proposed by Griffanti et al. [2]. The classification relied on three principal features: spatial distribution, temporal profile, and spectral content. Signal components were typically characterized by large, structured clusters located in grey matter regions with smooth time series and power spectra dominated by low-frequency oscillations. In contrast, noise components tended to be spatially fragmented, often located in white matter, CSF, or peripheral regions, with abrupt signal changes or flat spectral profiles indicating scanner noise, motion artifacts, or physiological interference. Examples include cerebrospinal fluid pulsations aliased into the BOLD frequency range, and susceptibility artifacts that appear near air-tissue interfaces. To validate the classification of signal components, the spatial maps were compared with canonical resting-state networks described in Smith et al. [3]. Overlaps were assessed visually using FSLeyes by overlaying the ICA components onto the MNI template and comparing them with RSN maps. Signal components showing high spatial correspondence with known networks such as the default mode network, visual network, or sensorimotor network were retained for further analysis, while noise components were discarded.

III. RESULTS

From the independent component analysis in MELODIC, there were obtained 49 components to classify in FSLeyes. Many components were discarded because they were inadequate, contained noise, or represented sources of disturbance, while others were excluded because they did not match the 10 maps of Smith et al.'s resting-state networks. The first component corresponds to the medial visual area (Figure 1.1). The second component corresponds to the occipital pole (Figure 1.2). The third component corresponds to the lateral visual area (Figure 1.3). The fourth component involves the medial parietal region (precuneus and posterior cingulate cortex), the bilateral inferior-lateral-parietal areas, and the ventromedial prefrontal cortex, corresponding to the default mode network (Figure 1.4). The fifth component covers the cerebellum (Figure 1.5). The sixth component includes the supplementary motor area, the primary sensorimotor cortex, and the secondary somatosensory cortex (Figure 1.6). The seventh component involves the superior temporal gyrus and posterior insular region, corresponding to the auditory network (Figure 1.7). The eighth component includes medial frontal areas, such as the anterior cingulate and paracingulate cortex (Figure 1.8). The ninth and tenth components represent the left and right frontoparietal networks, respectively (Figures 1.9 and 1.10). Other components were discarded because they represented noise. In Figure 2, the first image represents a motion artefact localized along the brain edges (Figure 2.1). The second image corresponds to physiological noise, likely related to cardiac or respiratory fluctuations (Figure 2.2). The third and fourth images represent physiological artefacts centered on the brainstem and vascular noise (Figures 2.3 and 2.4). Additional noise components were identified: another brainstem-related physiological artefact (Figure 2.5), scanner noise with minor motion artefacts (Figure 2.6), physiological and scanner-related noise (Figure 2.7), and superficial motion artefacts along the brain surface (Figure 2.8).

Figure 1. The images represent ICA signal components classified as resting-state networks, overlaid on the MNI template in sagittal, coronal, and axial planes.
Figure 2. The images represent ICA components classified as noise or artefacts, overlaid on the MNI template

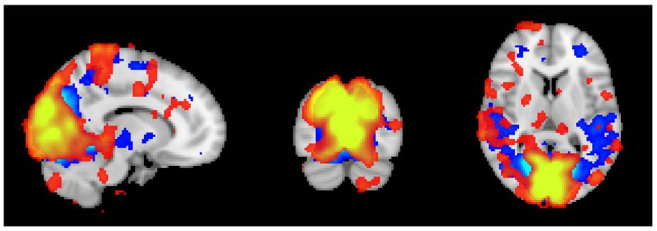

[1.1]

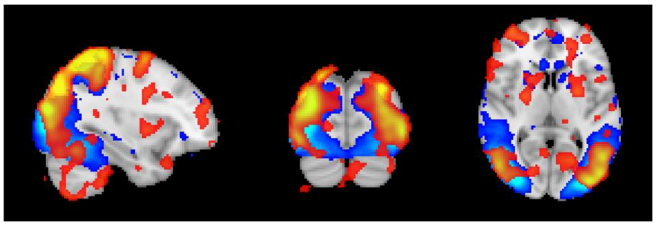

[1.2]

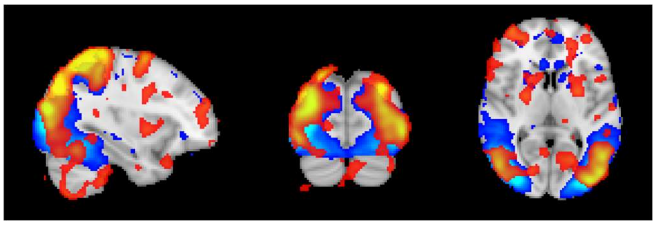

[1.3]

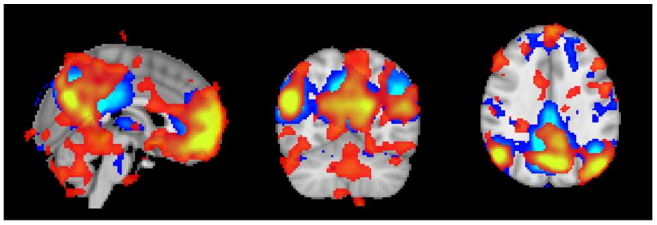

[1.4]

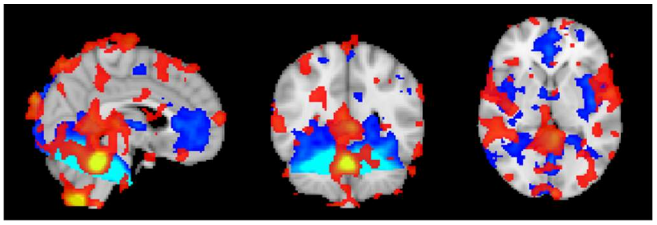

[1.5]

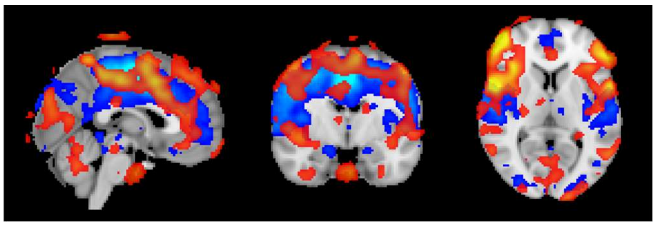

[1.6]

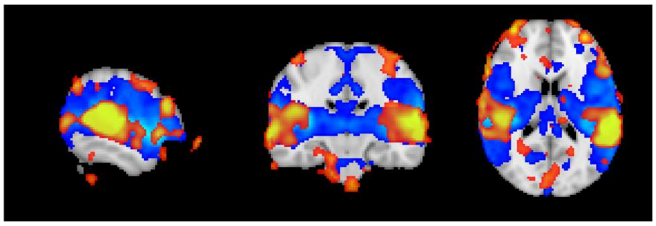

[1.7]

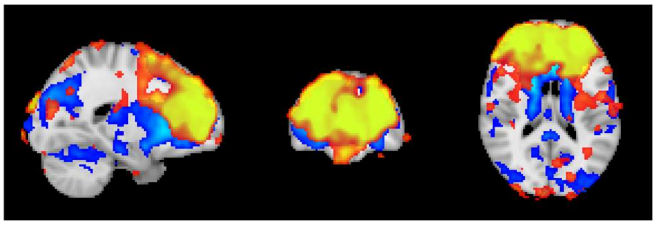

[1.8]

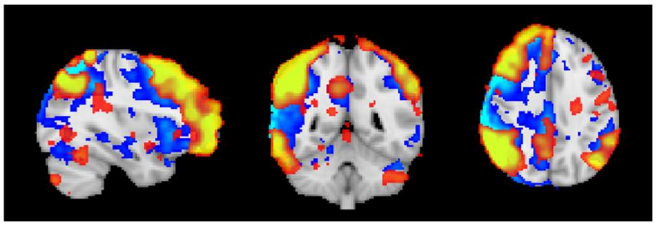

[1.9]

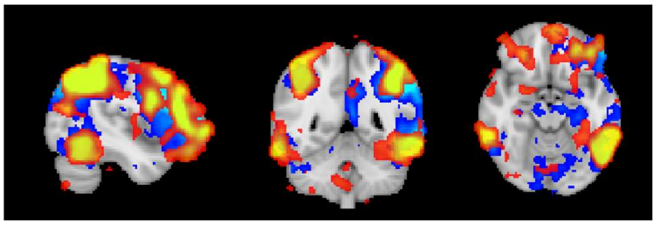

[1.10]

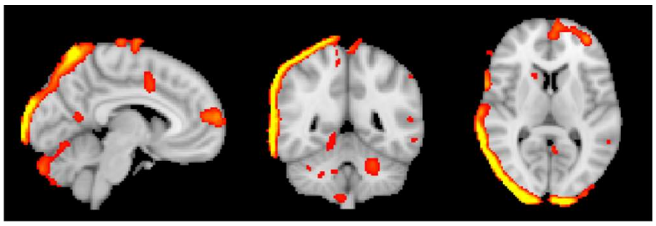

[2.1]

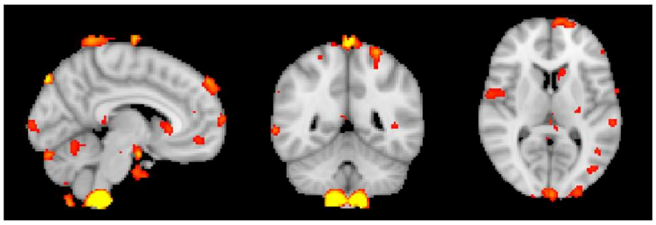

[2.2]

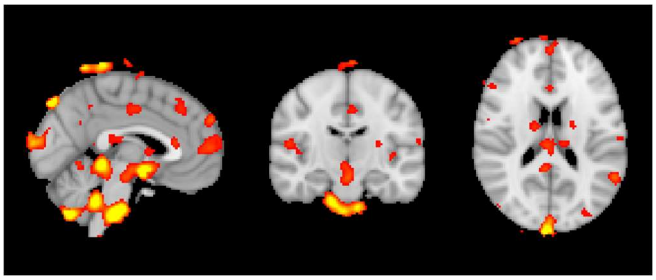

[2.3]

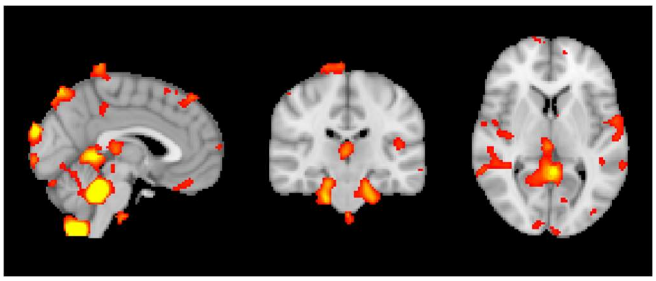

[2.4]

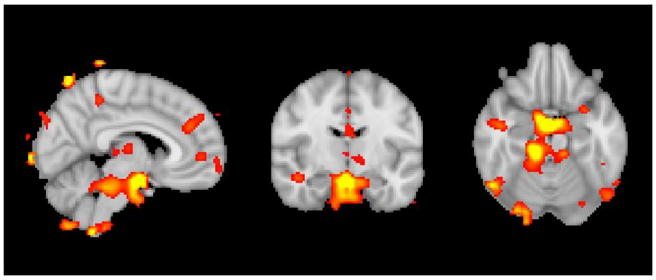

[2.5]

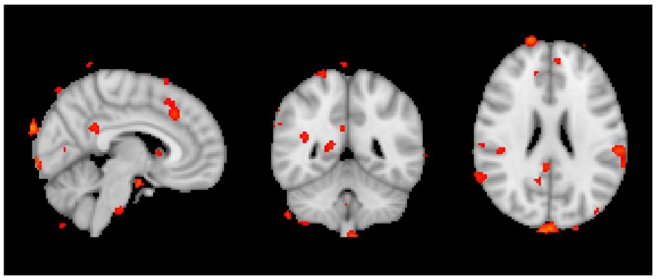

[2.6]

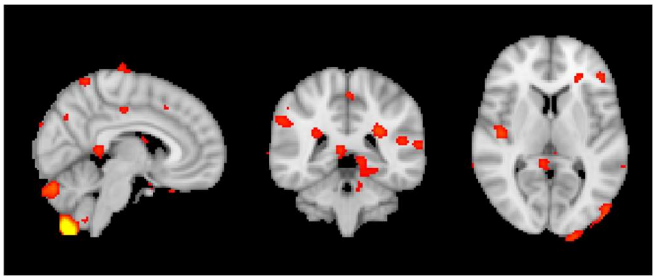

[2.7]

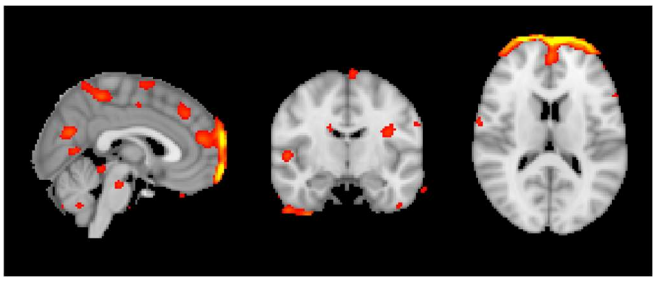

[2.8]

IV. DISCUSSION

In this study, independent component analysis (ICA) was used to extract 49 spatial components from resting-state fMRI data. Following the methodology proposed by Smith et al. (2009) and Griffanti et al. (2017), components were classified as either true resting-state networks (RSNs) or noise-related artefacts based on spatial, spectral, and temporal features. A key step in the classification involved the visual comparison between the ICA spatial maps and the canonical RSN templates defined by Smith et al. Overlapping the ICA components with Smith's RSNs provides a robust qualitative method to identify meaningful neural networks.

This comparison is crucial because true RSNs should display coherent and anatomically plausible activation patterns, corresponding to known functional systems, while noise components generally show sparse, random, or artefactual patterns. In this process, the ICA z-maps brightness and contrast were thresholded (min 2, max 11 respectively) as for Smith's RSN templates, which were overlaid to the latter (thresholds: min 2, max 6) to facilitate visual matching. In the current classification, 10 components (Figures 1.1 to 1.10) showed good spatial correspondence with Smith's RSNs, satisfying the expected anatomical and functional patterns. Specifically, the medial visual area (Figure 1.1), the occipital pole (Figure 1.2), and the lateral visual area (Figure 1.3) were well matched to the visual networks described by Smith. The default mode network (DMN, Figure 1.4) included the precuneus, posterior cingulate, bilateral inferior parietal lobules, and ventromedial prefrontal cortex, consistent with Smith's and Griffanti's definitions. The cerebellar network (Figure 1.5) was identified, although limited inferior cerebellar coverage was noted, a common limitation reported by Smith et al. due to field-of-view constraints. Similarly, the sensorimotor (Figure 1.6), auditory (Figure 1.7), and medial frontal (anterior cingulate) networks (Figure 1.8) showed acceptable overlap with canonical RSNs. The left and right frontoparietal networks (Figures 1.9 and 1.10) were clearly lateralized, consistent with the lateralization patterns reported in previous RSN studies. These results confirm that the selected ICA components correspond well to known resting-state networks, supporting the reliability of the visual classification method. Conversely, several components were classified as noise based on the guidelines by Griffanti et al. The spatial features of these noise components varied, but common characteristics were observed. Motion artefacts were identified through the presence of thin rings of activation along the cortical surface, as seen in Figures 2.1 and 2.9. Physiological artefacts, most likely related to cardiac and respiratory fluctuations, were distinguished by strong activations localized in the brainstem and deep brain regions, corresponding to Figures 2.2, 2.3, 2.4, and 2.5. Some components, such as those in Figures 2.6 and 2.7, exhibited low-intensity, randomly distributed activation patterns without a coherent anatomical organization, indicative of scanner-related noise. In other cases, components displayed a mixture of features, combining minor motion artefacts with physiological noise, complicating their classification but still fitting the criteria for noise exclusion. Identifying and discarding noise components is essential to ensure the integrity of resting-state fMRI analyses. As emphasized by Smith et al., true RSNs should demonstrate anatomically plausible, functionally interpretable spatial patterns, while noise components often reflect non-neuronal sources and must be excluded to avoid spurious findings. Griffanti et al. further highlighted the importance of considering not only spatial features but also the temporal characteristics (such as the smoothness of the time series) and the spectral content (with true RSNs generally associated with dominant low-frequency fluctuations).

V. CONCLUSION

This study demonstrated that independent component analysis (ICA), combined with visual classification based on established spatial, temporal, and spectral criteria, is an effective method for distinguishing true resting-state networks (RSNs) from noise in resting-state fMRI data. By systematically comparing the spatial maps of the extracted components with Smith et al.'s canonical RSNs, and by following the classification guidelines proposed by Griffanti et al., a reliable distinction between neural and artefactual components was achieved. The results confirmed that a substantial portion of the extracted components corresponded to meaningful RSNs, including well-recognized networks such as the medial and lateral visual networks, the default mode network, the sensorimotor and auditory networks, and the executive control networks. At the same time, several components were identified as noise, exhibiting characteristics consistent with motion artefacts, physiological fluctuations, and scanner-related disturbances. The rigorous classification of components is critical to ensure the validity of resting-state fMRI analyses, as the inclusion of noise components can compromise the

interpretability and reliability of the results. This work reinforces the importance of integrating visual inspection with template-based matching to enhance the quality of resting-state studies. Future work may further benefit from combining manual classification with automated denoising algorithms, promoting even greater standardization and reproducibility across studies.

REFERENCES

1. Smith, S. M., et al. (2009). *Correspondence of the brain's functional architecture during activation and rest*. Proceedings of the National Academy of Sciences, 106(31), 13040–13045.
2. Griffanti, L., et al. (2017). *Hand classification of fMRI ICA noise components*. NeuroImage, 154, 188–205.
3. Salimi-Khorshidi, G., et al. (2014). *Automatic denoising of functional MRI data: combining independent component analysis and hierarchical fusion of classifiers*. NeuroImage, 90, 449–468.
4. OpenNeuro Dataset: *Yale Resting State fMRI/Pupillometry: Arousal Study*. Available at: https://openneuro.org/datasets/ds003768
5. Lee, M. H., Smyser, C. D., & Shimony, J. S. (2013). *Resting-state fMRI: a review of methods and clinical applications*. AJNR Am J Neuroradiol, 34(10), 1866–1872.
6. Morgan, V. L., Dawant, B. M., Li, Y., & Pickens, D. R. (2007). *Comparison of fMRI statistical software packages and strategies for analysis of images containing random and stimulus-correlated motion*. Computerized Medical Imaging and Graphics, 31(6), 436–446.
7. Snyder, A. Z., & Raichle, M. E. (2012). *A brief history of the resting state: the Washington University perspective*. NeuroImage, 62(2), 902–910.